



RESEARCH PAPER

OPEN ACCESS

Isotherm Modeling and Thermodynamic Investigation of Mercury Adsorption on Functionalized Carbon Nanotubes: A Comparative Study of SWCNTs and MWCNTs

Received:

2026/01/04

Accepted:

2026/02/26

Published:

2026/03/01

Nupur Garg¹ and Kiran Jeet² ¹Department of Mathematics, Statistics & Physics, Punjab Agricultural University, Ludhiana- 141004, India²Electron Microscopy and Nanoscience Laboratory, Punjab Agricultural University, Ludhiana- 141004, India

*Correspondence for materials should be addressed to KJ (email: kiranjeet@pau.edu)

Abstract

This study presents the surface modification of carbon nanotubes (CNTs) to investigate their efficacy as adsorbents for the removal of mercury (Hg(II)) from aqueous solutions. Thiol groups were conjugated to the open ends of CNTs using a series of carboxylation, reduction, chlorination, and thiolation reactions. The functionalization of carbon nanotubes (CNTs) was validated by Fourier Transform Infrared (FT-IR) Spectroscopy, Transmission Electron Microscopy (TEM), and Scanning Electron Microscopy (SEM). The capacity of surface modified CNTs to remove Hg (II) was investigated in relation to many factors, including adsorbent dose, contact duration, pH, and system temperature. Thiol-functionalized CNTs exhibited superior adsorption of Hg (II) ions relative to carboxylic-functionalized CNTs. The computed values of thermodynamic parameters, including enthalpy change (ΔH_0) and entropy change (ΔS_0), were found to be positive, indicating that the adsorption of mercury ions on the surface of CNTs is an endothermic process. The adsorption capacity of all adsorbents was examined using equilibrium isotherms, namely Langmuir and Freundlich, revealing that the highest adsorption capacity was recorded for thiol-functionalized single-walled carbon nanotubes, followed by thiol-functionalized multiwalled carbon nanotubes.

Keywords: Carbon Nanotubes; Mercury (Hg (II)); Adsorption; Water Decontamination; Isotherms; Thermodynamics

Introduction

The rapidly reduction of clean water sources, diminishing surface water levels, wastewater pollution, and environmental contamination by toxic substances have emerged as the most critical issues confronting our planet in the twenty-first century. The elimination of inorganic and organic pollutants from water is regarded as one of the foremost challenges in recent decades. The primary sources of water contamination include wastewater runoff and industrial discharges containing dyes, pesticides, fertilizers, hazardous chemicals, and heavy metals.

Among the heavy metal contaminants, elemental mercury is considered to be carcinogenic to humans and high exposure to Hg (II) compounds may even cause death (Pacyna et al., 2010). The most common natural source of Hg (II) is from volcanic eruptions, which result in about 50% of the atmospheric Hg (II) emissions.



However, anthropogenic sources such as coal plants, gold manufacturing, non-ferrous metal smelters, cement production industry, pig iron and steel production industry, chlor-alkali industry and battery industry have also led to elevated levels of Hg (II) in the environment (Pacyna et al., 2010). Various regulatory bodies have set maximum prescribed limits for the discharge of toxic heavy metals into the aquatic systems. World Health Organization (WHO) has recommended a maximum acceptable concentration of $1\mu\text{g/L}$ in drinking water (Puri and Kumar, 2012). However, the metal ions are being added to the water stream at a much higher concentration than the prescribed limits by industrial activities, thus leading to health hazards and environmental degradation.

In recent years, diverse treatment methods have been used to remove Hg(II) from wastewater based on chemical precipitation, adsorption, ion exchange, membrane separation and electrochemical processes (Chen et al., 2018; Khan et al., 2015; Kumar et al., 2017; Matlock et al., 2001; Pothitontimongkol et al., 2009; Rezvani-Boroujeni et al., 2015; Samani et al., 2016; Zeng et al., 2021). Adsorption is recognized as one of the most promising technologies for large-scale applications because of its economic effectiveness, flexibility in operation, and possibility of regeneration (Ahmad et al., 2025; Burakov et al., 2018; Dhoble et al., 2018; Loganathan et al., 2014; Peng et al., 2017).

Activated carbon serves as an adsorbent; nevertheless, it is ineffective at low metal ion concentrations and generates waste products that are challenging to dispose of in an environmentally responsible manner, in addition to lacking selectivity for certain metal ions. Additional downsides include inadequate metal extraction, substantial reagent and energy demands, and the production of hazardous sludge or other waste materials necessitating meticulous disposal (Yardim et al., 2003). Consequently, there is significant scientific interest in creating an adsorbent that has high efficiency and selectivity for the removal of Hg ions.

A variety of carbon based nanomaterials have been engineered to eliminate heavy metals from aquatic environments due to their distinctive electrical, mechanical, thermal, optical, and chemical capabilities. These materials possess a high surface area and have distinctive properties for adsorption applications. The use of carbon nanotubes (CNTs) in adsorption is constrained by their inadequate dispersion in solvents, attributable to the robust intermolecular interactions among the nanotubes. The adsorption capacity of carbon nanotubes can be enhanced by the introduction of novel functional groups by acid oxidation.

Nonetheless, oxidized CNTs exhibit limited metal ion absorption from aqueous solutions, necessitating further functionalization to selectively target particular metal ions in aquatic environments. Therefore, to employ carbon nanotubes in diverse applications, their architectures are frequently modified to align with the individual requirements. Carbon nanotubes (CNTs) have demonstrated exceptional adsorption properties for various divalent metal ions in aqueous solutions due to their capacity to form π - π electrostatic interactions. The sorption capacity of CNTs is mostly associated with the functional groups affixed to their surface. The presence of functional groups on the surface of carbon nanotubes enhances reactivity and offers active sites for further chemical changes (Abraham et al., 2012).

This work examines the thiol and carboxylic functionalization of carbon nanotubes to enhance their selectivity for mercury ion adsorption. A thorough investigation is conducted on the adsorption of Hg (II) ions onto functionalized single-walled carbon nanotubes (SWCNTs) and functionalized multi-walled carbon nanotubes (MWCNTs). The adsorption equilibrium data were analyzed by fitting them into several isotherm models to ascertain design objectives.

Experimental Details

Functionalisation and Characterisation of CNTs

Pristine SWCNT and MWCNT powders (SRL, India) were oxidized with 3 M nitric acid via sonication (2 h, 80 °C) and reflux (24 h, 80–90 °C), followed by neutralization and filtration to obtain carboxyl-functionalized CNTs (CNT–COOH) (Kar and Choudhury 2013). Thiol groups were introduced by treating CNT–COOH with thionyl chloride/DMF (24 h, 80 °C), followed by NaOH, ethanol, and HCl washing, yielding thiol-functionalized CNTs (CNT–SH) (Lim et al., 2003).

Six samples were prepared: pristine SWCNT, SWCNT–COOH, SWCNT–SH, pristine MWCNT, MWCNT–COOH, and MWCNT–SH and tested for adsorption of Hg (II) ions. The Hg (II) concentration was measured by a UV-visible spectrophotometer (Elico SL 159 model) using a standard method (Gowenlock and Trotman 1955). Functionalization was confirmed by FTIR (Thermo Nicolet 6700), while morphology was examined by TEM (Hitachi H-7650) and SEM (Hitachi S-3400 N).

Adsorption studies

A 100 mg/L Hg(II) stock solution was prepared from mercury dichloride (HgCl₂) in ethanol and diluted to obtain working solutions (5–50 mg/L). Adsorption experiments with six CNT adsorbents were conducted under varying pH, contact time, dosage and temperature. Mercury concentrations were measured at 215 nm, and removal efficiency was calculated from initial and final concentrations (Hadavifar et al., 2014).

$$\text{Percentage Removal} = \frac{C_i - C_f}{C_i} \times 100 \quad (1)$$

Where C^i initial metal concentration (mg/l) and C^f final metal concentration (mg/l). The change in free energy ΔG° , enthalpy ΔH° and entropy ΔS° associated with the adsorption process were calculated using the following equations:

$$\begin{aligned} \Delta G^\circ &= -RT \ln K \\ \ln K &= -\frac{\Delta H^\circ}{RT} + \frac{\Delta S^\circ}{R} \end{aligned} \quad (2)$$

Where R is the gas constant (8.314 J/mol/K), T is the absolute temperature (K), K (q_e/C_e) an equilibrium constant at various temperatures (Mobasherpour et al., 2014). ΔH° and ΔS° were calculated from the slope and intercept of the plot of $\ln K$ vs $1/T$.

Results and Discussion

Characterization

Figures 1 (a) and (b) provide a comparison of the FT-IR spectra for pure, oxidized, and thiolated SWCNTs and MWCNTs, respectively. A peak at around 3400 cm⁻¹ corresponds to the O-H stretching vibration of the hydroxyl group. A peak at 2923.2 cm⁻¹ in the spectra of pristine samples was observed, indicative of C-H stretching vibrations (Verma, 2015), whereas a peak at 2852.8 cm⁻¹ corresponds to C-H bending (Rizwan, 2010). The C-O bands about 1000 cm⁻¹ were seen in all three spectra, attributed to ketones or quinones, or maybe linked to the aromatic C=C stretching inside the graphene structure. The IR spectra of oxidized CNTs include four prominent peaks at 1740, 1635.5, 1556.5, and 1532.9 cm⁻¹. The peaks signify the binding of carboxylic groups to the surface of pure CNTs. The peaks at 1532.9 and 1145 cm⁻¹ in the spectra of oxidized CNTs correspond to the asymmetric and symmetric stretching of C-O-C bonds, respectively (Rizwan, 2010). The new peak at 1384.3 cm⁻¹ corresponds to the deformation vibration of CH₂ groups. The peak at 1641.4 cm⁻¹ in SWCNT and 1637.6 cm⁻¹ in MWCNT spectra clearly indicates the presence of thiol groups on the surface of CNTs (Luqman et al., 2009).

The SEM pictures of both SWCNTs and MWCNTs in their pristine condition (Figure 2) exhibit entangled tubes, while the SEM micrographs of functionalized CNTs reveal well-ordered, locally aligned tubes. The aggregation of pristine CNTs can be ascribed to intermolecular forces among CNTs of varying sizes and orientations. The formation of functional groups on nanotube surfaces produces a repulsive force that causes debundling of the nanotubes, therefore increasing their surface area. The nanotubes undergo shortening upon oxidation under extreme experimental conditions.

TEM micrographs (Figure 3) indicate that a greater quantity of amorphous carbon is produced in MWCNTs compared to SWCNTs, attributable to the stability of SWCNTs relative to MWCNTs. In multi-walled carbon nanotubes (MWCNTs), the existence of dangling bonds in neighbouring shells intensifies intershell covalent bonding under severe functionalization conditions, resulting in the creation of increased amorphous carbon in the sp³ state. No substantial alterations in structure are noted for both thiol and carboxylic functionalized carbon nanotubes.

Adsorption studies

Batch adsorption tests were conducted to evaluate the efficacy of several adsorbents (SWCNTs, SWCNT-COOH, SWCNT-SH, MWCNT, MWCNT-COOH, and MWCNT-SH) in the removal of Hg (II) ions from water/aqueous medium.

Effect of adsorbent dose

Figure 4(a) illustrates a comparison of the six adsorbents (pristine SWCNT, SWCNT-COOH, SWCNT-SH, pristine MWCNT, MWCNT-COOH, MWCNT-SH) at three distinct dosages (1 mg, 1.5 mg, and 2 mg). The results indicate that SWCNT-SH had superior adsorption behavior compared to the other adsorbents. It was shown that an increase in adsorbent dose correlates with a higher percentage of ion removal, attributable to the augmented availability of new sites on the adsorbent surface. No other metal establishes a robust covalent connection with a thiol functional group as effectively as the mercury ion (200 kJ/mol). Thiol groups bond to alkyl chains, imparting significant flexibility to allow a linear S-Hg-S configuration. The experiment demonstrated that the highest removal of Hg (II) ions from aqueous solution was 91.83% and 90.71% for SWCNT-SH and MWCNT-SH, respectively, achieved at a

concentration of 0.4 mg/ml of the respective CNT samples. Functionalized SWCNTs have superior adsorption properties compared to functionalized MWCNTs due to the increased generation of amorphous carbon in MWCNTs, as SWCNTs demonstrate more stability than MWCNTs.

The removal percentage of Hg (II) ions using carboxylic functionalized MWCNTs was 85.39%, which is lower than the 90.71% achieved with thiol functionalized MWCNTs. This discrepancy is attributed to the low charge density of Hg (II) ions, which are classified as soft acids that establish robust covalent bonds with soft bases like sulfur (Blue et al., 2010). Oxidized CNTs exhibited adsorption due to the reaction of carboxylic groups created on their surface with bases, resulting in the formation of ionic salts, which are soluble in water (Atieh et al., 2010).

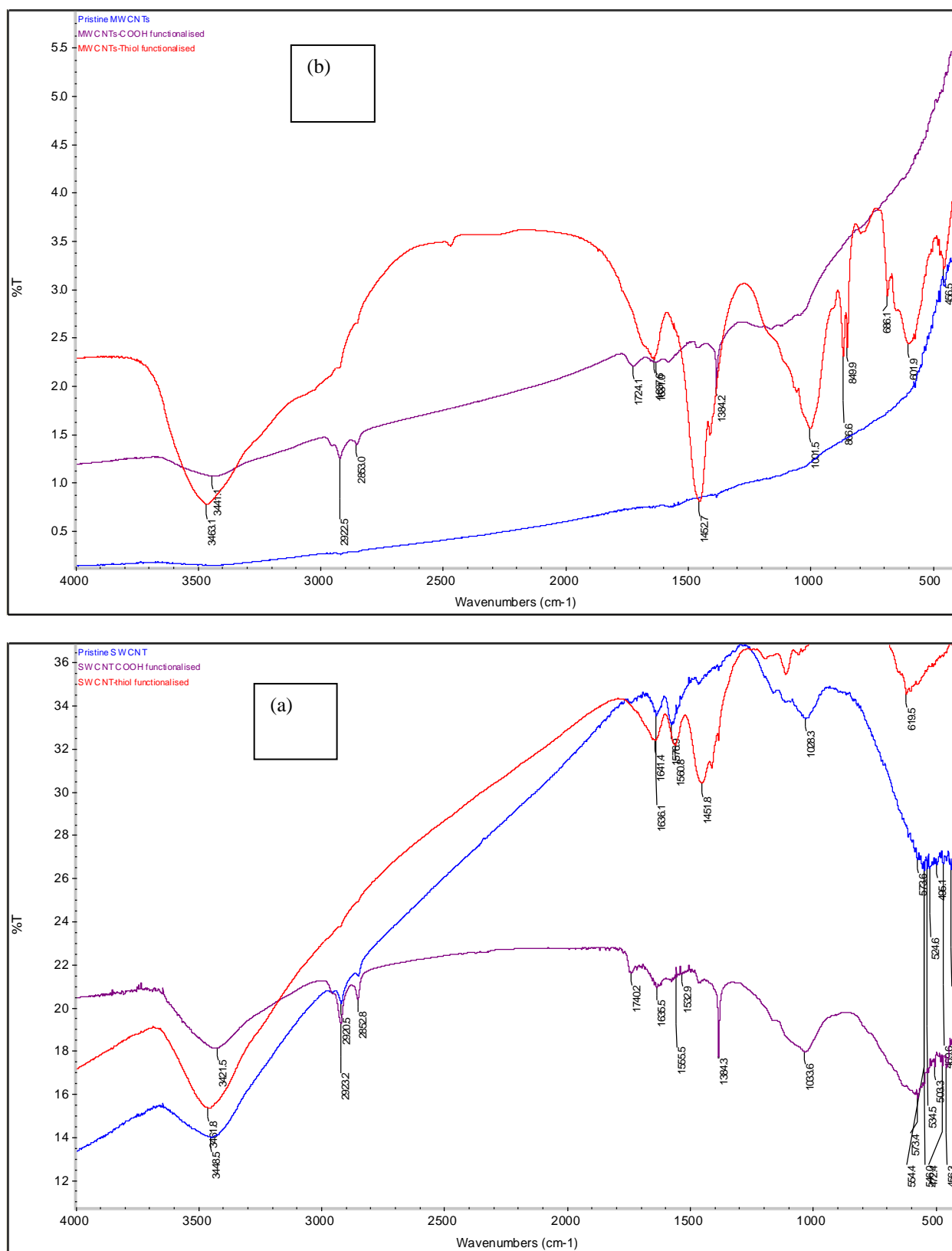
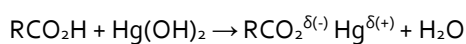


Fig. 1. Fourier Transform Infrared (FT-IR) spectra of pristine, carboxylic and thiol functionalized (a) SWCNTs and (b) MWCNTs



The unmodified SWCNTs and MWCNTs exhibited significantly lower adsorption rates of 59.24% and 63.41%, respectively, at the same adsorbent dosage. Trends indicated the ideal adsorbent dose of both SWCNT and MWCNT for the efficient removal of mercury from aqueous solutions. As the dose of the adsorbent grows, the percentage removal rises, while the adsorption density diminishes, given a constant starting concentration of mercury ions. This phenomenon may be attributed to the presence of unsaturated adsorption sites throughout the adsorption process (Bandaru et al., 2013) indicated that to achieve total saturation of the adsorbent surface with mercury ions, elevated concentrations of the adsorbent should be avoided.

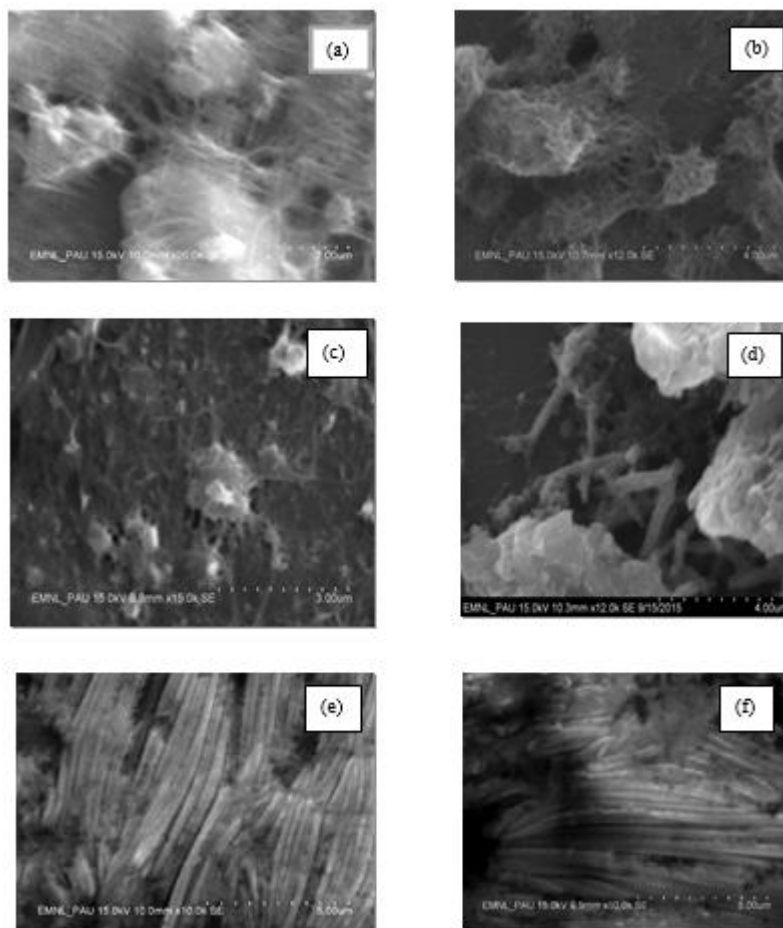


Fig. 2. Scanning Electron micrographs of (a) Pristine SWCNT, (b) Pristine MWCNT, (c) SWCNT-COOH, (d) MWCNT-COOH, (e) SWCNT-SH and (f) MWCNT-SH.

Effect of contact time

Figure 4 (b) illustrates the variation in adsorption capacity of the adsorbent with respect to differing contact times between the adsorbent and the metal ion Hg (II) in aqueous solution. Within a duration of 2 hours, SWCNT-SH exhibits a maximum mercury (II) removal percentage of 90.42%, whereas MWCNT-SH demonstrates a removal percentage of 89.27%. In the plots of MWCNT-COOH, MWCNT-SH, and SWCNT-SH, quick adsorption was seen, likely attributable to the greater availability of unoccupied binding sites. However, as contact time increased, the remaining sites were increasingly challenging to fill due to repulsive interactions between the adsorbate ions on the solid and those in solution. Pristine samples possess a higher surface area; yet, they exhibit little adsorption relative to functionalized samples due to their hydrophobic characteristics. The removal percentages of Hg (II) ions for pure SWCNTs and MWCNTs are 57.84% and 61.22%, respectively, but carboxylic functionalized samples exhibit substantially higher removal percentages. SWCNT-COOH eliminated 88.05% of mercury ions, whereas MWCNT-COOH removed 80.21% of mercury ions from the aqueous solution. The slope of the curves increases in the initial half and then maintains a steady trend due to the extended duration for the interaction of mercury ions with the surface of carbon nanotubes (CNTs).

Effect of pH

The influence of pH (varying from 2 to 10) on the adsorption capacity of both pure and functionalized carbon nanotubes was examined while maintaining a constant temperature of 25°C. All adsorbents demonstrate a rise in the % removal of Hg (II) with rising pH values, as seen in Figure 4 (c). Figure 4 (c) indicates that at pH 10.2, thiol-

functionalized SWCNT exhibits a mercury (II) removal percentage of 91.14%, while MWCNT demonstrates 88.41%. The carboxylic-functionalized samples reveal removal percentages of 88.3% for SWCNT and 70.35% for MWCNT, respectively. Pristine samples of SWCNT and MWCNT exhibit only 57.58% and 62.01% clearance of Hg from the aqueous sample, respectively. The percentage of adsorption rises linearly up to pH 6.0, exhibiting a negligible improvement in the removal of Hg (II) ions at pH levels beyond 6. Despite observing a maximum Hg (II) ion percentage of 91.14% for thiol-functionalized SWCNTs at pH 10.2, the studies were done at pH 6.0 to mitigate the influence of mercury hydroxide.

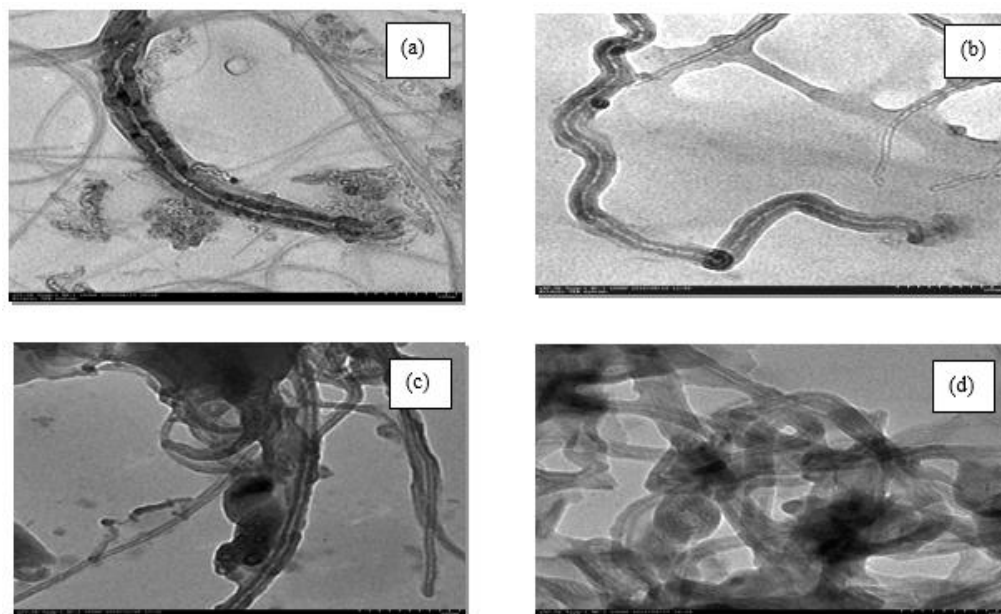
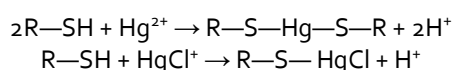


Fig. 3. Transmission Electron micrographs of (a) SWCNT-COOH, (b) MWCNT-COOH, (c) SWCNT-SH and (d) MWCNT-SH

The surface charge of the adsorbent (CNTs) markedly affected the adsorption process of Hg (II) ions. The little adsorption seen in the acidic region may stem from unfavorable electrostatic interactions. As pH rises, the surface charge of CNTs becomes increasingly negative, enhancing advantageous electrostatic interactions. This enables lone pairs of electrons on oxygen or sulfur to engage with mercury ions on the surface, leading to improved adsorption of metal species (Stafiej and Pyrzynska, 2007). The interactions between thiol and Hg(II) ions as soft acids and soft bases significantly enhance adsorption at pH values over 5.0. The reaction mechanism of the —SH functional group with mercury ion species is outlined by the following equations (Hosseini et al., 2013):



The aforementioned reactions demonstrate that an increase in the concentration of OH⁻ ions results in greater consumption of H⁺ ions in the solution, facilitating the appropriate progression of the reaction.

Effect of temperature

Figure 4 (d) illustrates that as temperature rises; the percentage removal capabilities of the adsorbent samples increase. This signifies that heat enhances the adsorption process. The elimination percentage increases by roughly 2% as the temperature escalates from 25°C to 30°C for SWCNT-SH samples and by 7% for MWCNT-SH samples. The elimination percentage increases by roughly 7.3% as the temperature rises from 25°C to 35°C for SWCNT-SH samples and by 20% for MWCNT-SH samples. The highest % removal of mercury was achieved at 35°C for all adsorbents, exhibiting a linear trend.

Thermodynamic parameters

The adsorption data collected at three distinct temperatures was utilized to assess the thermodynamic parameters of the adsorption process. The values of ΔH_0 and ΔS_0 were derived from the slope and intercept of the $\ln K$ against $1/T$ plot (figure 5). The rise in $\ln K$ with rising temperature (Table 2) indicates that the process is endothermic. The data from Figure 5 yielded positive values of ΔS_0 (Table 1), signifying an increase in the randomness of the solid solution interface system during the adsorption process. Positive values of ΔH_0 suggest that the adsorption of mercury (II) ions onto the surface of CNTs is endothermic, a conclusion corroborated by the rise in mercury ion adsorption with rising temperature. Lower values of ΔG_0 indicate that adsorption became more spontaneous at elevated temperatures. Shadbad et al. (2011) obtained same findings for thermodynamic parameters.

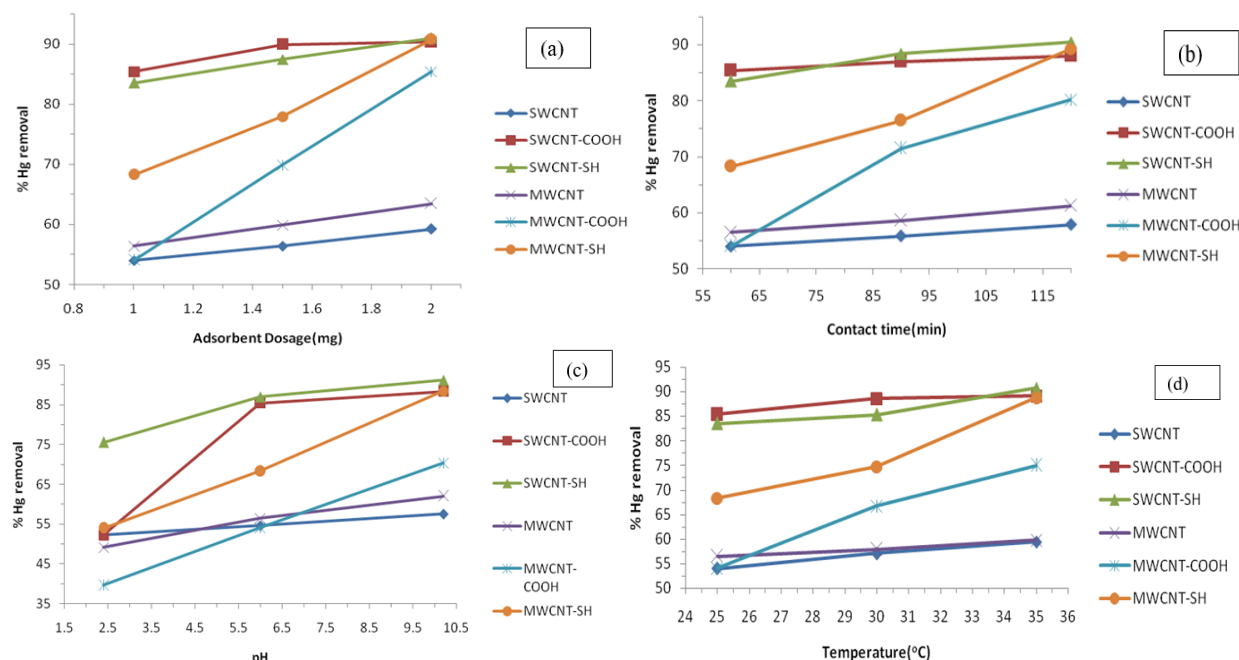


Fig. 4. Effect of (a) adsorbent dose (at 25°C), (b) contact time (at 25°C), and (c) pH (at 25°C) and (d) temperature (25°C -35°C) on Hg (II) adsorption at 25°C using pristine and functionalized CNTs

Adsorption Isotherm study

The adsorption isotherm is essential for elucidating the interaction between solutes and adsorbents, and it is pivotal for optimizing the application of adsorbents. Adsorption isotherms delineate the equilibrium distribution of metal ions between the liquid and solid phases (Tan and Hameed 2010). This study conducted an adsorption isotherm analysis using the Langmuir and Freundlich models. The Langmuir model is a theoretical framework, whereas the Freundlich isotherm is empirical in nature. The Langmuir model posits that at maximal coverage; a monomolecular layer exists on the surface. This indicates that absorbed molecules do not stack. The Freundlich isotherm imposes no such limitation. The Freundlich isotherm pertains to physical adsorption, whereas the Langmuir isotherm is relevant to chemisorption. The Langmuir isotherm signifies active surface adsorption on a homogeneous surface, whereas the Freundlich isotherm applies to heterogeneous surfaces (Rao et al., 2007).

Langmuir Isotherm

Theoretically, the Langmuir isotherm is typically employed to characterize the sorption of solute from a liquid solution as follows:

$$Q_e = \frac{q_m K_a C_e}{1 + K_a C_e} \quad (3)$$

The constant q_m and K_a are the characteristic of the Langmuir equation and can be determine from the linearised form as in Eq. (2) represented by:

$$\frac{C_e}{Q_e} = \frac{1}{q_m K_a} + \frac{C_e}{q_m} \quad (4)$$

Where C_e is the equilibrium Hg^{2+} ion concentration (mg/L), Q_e is the amount of Hg^{2+} adsorbed at equilibrium (mg/g) and q_m is Q_e for complete monolayer (mg/g) and K_a is sorption constant equilibrium constant (L/mg) (Dada et al., 2012). Langmuir model gives the specific surface coverage so it only allows the surface of a material to be used for sorption.

Langmuir isotherms were constructed for the adsorption of Hg (II) ions at varying concentrations (5, 10, 15, 20, 25, 30, 35, 40, 45, and 50 ppm) at 25°C, pH 6.0, a contact duration of 1 hr, and an adsorbent dosage of 1 mg for all adsorbents. In Langmuir adsorption isotherms, a linear isotherm was constructed between $1/C_e$ and $1/q_e$. All carbon nanotube samples yield a linear relationship, confirming that the data aligns adequately with the Langmuir model. The Langmuir plots for all CNT samples are presented in figures 6 (a) - (f).

The values of q_{max} and K_a have been derived from these plots and shown in Table 3. q_{max} represents the maximal adsorbate absorption under specified circumstances, whereas K_a is the coefficient associated with the affinity between the adsorbent and the adsorbate (Maleki et al., 2017). A steep incline in the Langmuir isotherms indicates that the adsorbent's capacity is elevated at low concentrations of Hg (II) ions, diminishing as the metal ion concentration increases due to the saturation of active sites on the adsorbent surface. The highest adsorption

capacity (q_m) derived from the Langmuir model is 111.12 mg/g for SWCNT-SH, followed by 83.34 mg/g for MWCNT-SH.

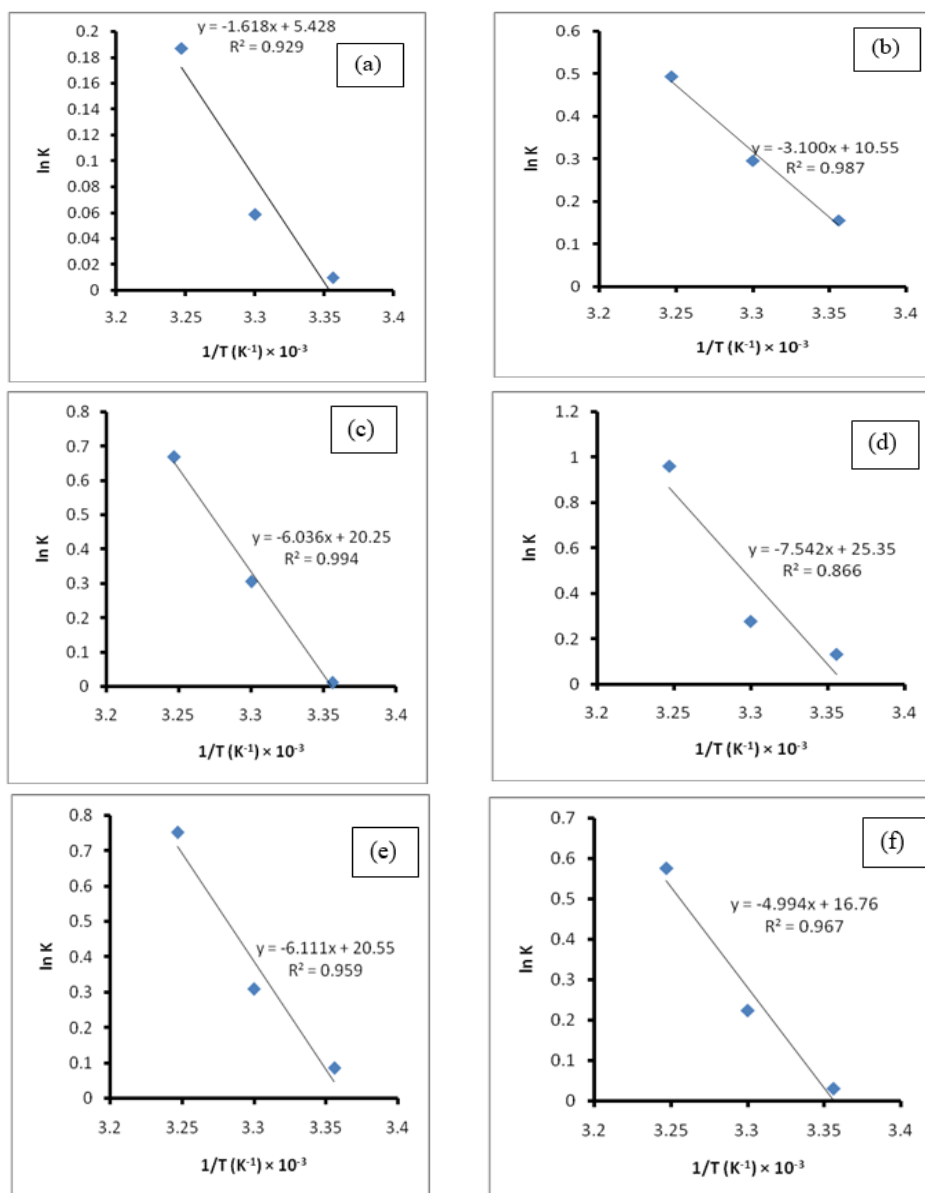


Fig. 5. Plot of $\ln K$ vs $1/T$ to predict thermodynamic parameters for the adsorption of Hg (II) ions onto (a) SWCNT (b) SWCNT-COOH (c) SWCNT-SH (d) MWCNT (e) MWCNT-COOH (f) MWCNT-SH

Freundlich Isotherm

The Freundlich isotherm is the earliest known relationship describing the sorption equation and is expressed by the following equation:

$$Q_e = K_F C_e^{\frac{1}{n}}$$

and the equation may be linearised by taking logarithms

$$\log(Q_e) = \frac{1}{n} \log(C_e) + \log(K_F)$$

Where C_e is the equilibrium Hg^{2+} ion concentration (mg/L), Q_e is the amount of Hg^{2+} absorbed at equilibrium (mg/g), K_F and $1/n$ are empirical constants dependent on several environmental factors (Dada et al., 2012). The Freundlich model gives the amount absorbed per unit mass of adsorbate.

Figure 7, presents the Freundlich plots. A plot of $\log C_e$ vs $\log Q_e$ yields a linear relationship for all carbon nanotube samples, indicating that the data adheres to the Freundlich equation as well. The Freundlich equation is an empirical formula, and the calculated parameters are presented in Table 4. The adsorbent's finite absorption capacity is not shown, limiting its application to low to intermediate concentration ranges, since homogeneous systems exhibit n values toward unity, while heterogeneous systems approach zero (Stafiej and Pyrzynska, 2007).

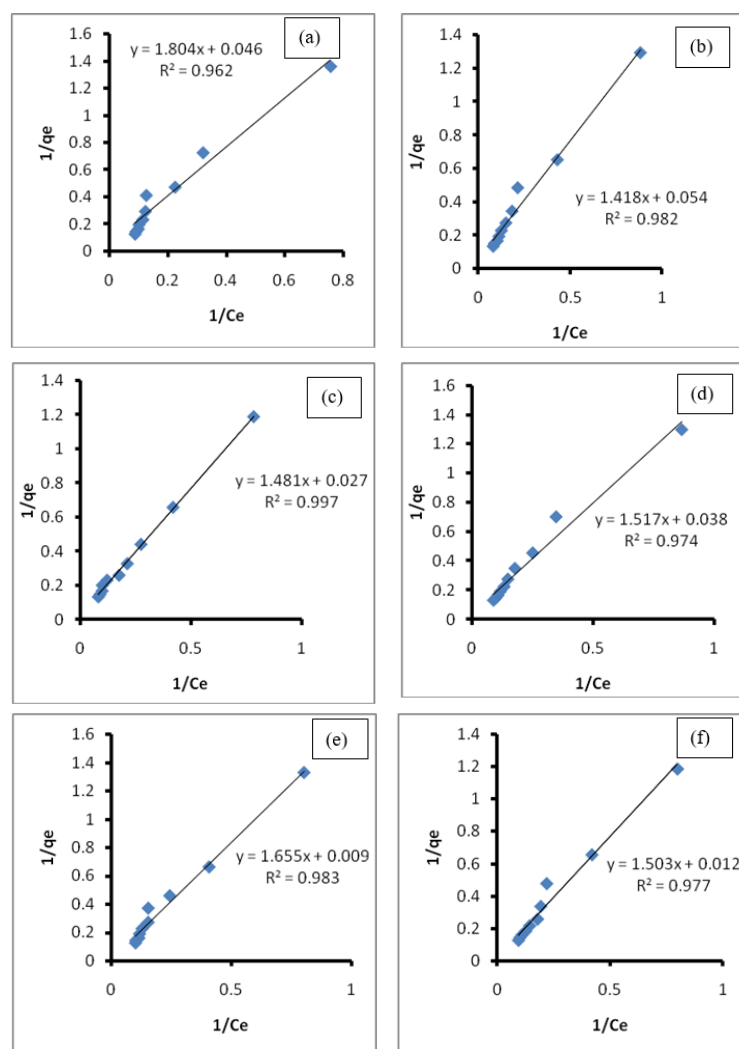


Fig. 6. Langmuir adsorption isotherm for Hg (II) ions adsorption on (a) pristine SWCNT, (b) pristine MWCNT, (c) SWCNT-COOH, (d) MWCNT-COOH, (e) SWCNT-SH, (f) MWCNT-SH

Table 1. Thermodynamic parameters (S° and H°) for Hg(II) ion adsorption

Adsorbent	SWCNT	SWCNT-COOH	SWCNT-SH	MWCNT	MWCNT-COOH	MWCNT-SH
$H^\circ(\text{kJmol}^{-1})$	13.452	25.773	50.183	62.704	50.807	41.520
$S^\circ(\text{kJmolK}^{-1})$	0.045	0.088	0.168	0.211	0.171	0.139

Table 2. (i) Thermodynamic parameters (G°) for Hg(II) ion adsorption for SWCNTs

Adsorbent	SWCNT		SWCNT-COOH		SWCNT-SH	
	$\ln K$ (img^{-1})	ΔG° (kJmol^{-1})	$\ln K$ (img^{-1})	ΔG° (kJmol^{-1})	$\ln K$ (img^{-1})	ΔG° (kJmol^{-1})
298	9.65	-23.90	155.94	-386.34	10.73	-26.59
303	58.65	-147.73	296.39	-746.66	305.42	-769.41
308	186.86	-478.49	494.53	-1266.34	669.46	-1714.28

(ii) Thermodynamic parameters (G°) for Hg(II) ion adsorption for MWCNTs

Adsorbent	MWCNT		MWCNT-COOH		MWCNT-SH	
	$\ln K$ (img^{-1})	ΔG° (kJmol^{-1})	$\ln K$ (img^{-1})	ΔG° (kJmol^{-1})	$\ln K$ (img^{-1})	ΔG° (kJmol^{-1})
298	134.81	-334.01	84.99	-210.59	29.89	-74.06
303	279.65	-704.49	309.14	-778.77	223.52	-563.08
308	962.05	-2463.54	753.34	-1929.08	575.87	-1474.63

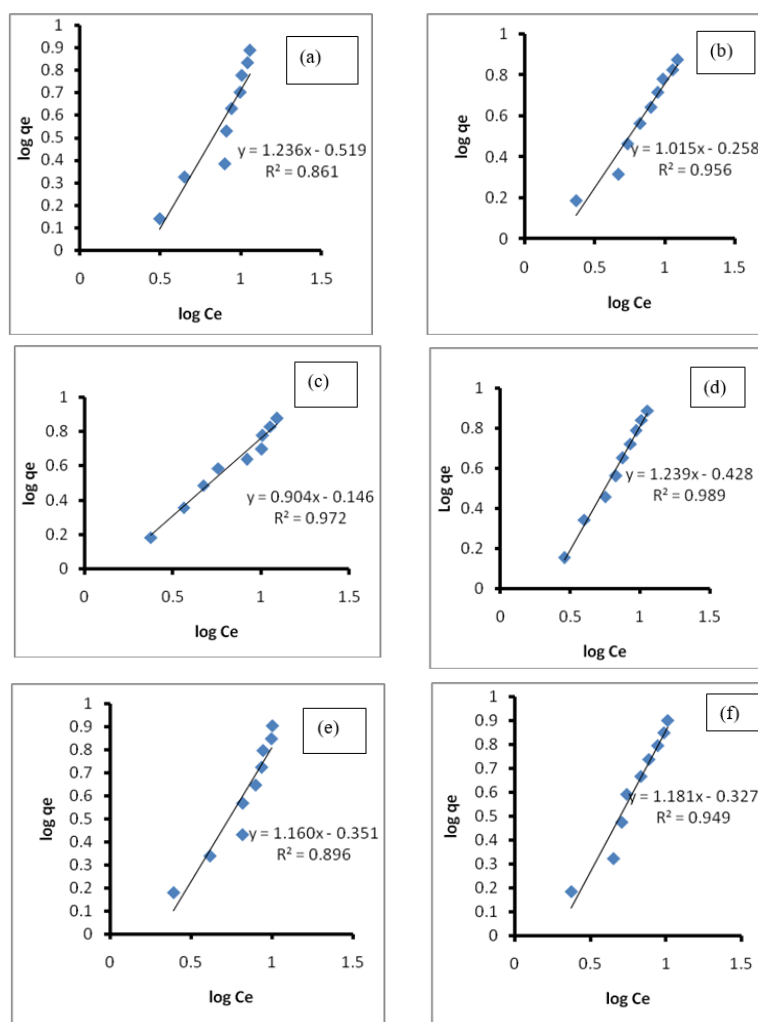
Table 3. Estimated Langmuir parameters for Hg(II) adsorption

Sample	SWCNT	SWCNT-COOH	SWCNT-SH	MWCNT	MWCNT-COOH	MWCNT-SH
$q_m(\text{mg/g})$	21.74	37.04	111.12	18.52	26.32	83.34
$K_a(\text{l/mg})$	0.026	0.018	0.005	0.038	0.025	0.008
R^2	0.962	0.997	0.983	0.982	0.974	0.977

Table 4. Estimated Freundlich parameters for Hg (II) adsorption

Sample	SWCNT	SWCNT-COOH	SWCNT-SH	MWCNT	MWCNT-COOH	MWCNT-SH
n	0.809	1.106	0.862	0.985	0.807	0.846
$K_f(\text{mg l}^{-1})$	0.595	0.864	0.704	0.773	0.651	0.721
R^2	0.861	0.972	0.896	0.956	0.989	0.949

Comparing the R^2 values from Tables 3 and 4 of estimated isotherm parameters reveals that the Langmuir isotherms provide a superior match to the experimental data of the CNT samples compared to the Freundlich isotherms. The Langmuir isotherm's validity indicates that adsorption occurs as a monolayer process, necessitating identical activation energy for the adsorption of mercury ions. The enhanced adsorption capacity of thiol-functionalized carbon nanotubes is attributable to the robust soft acid-soft base interactions between Hg (II) ions and the thiol groups on the nanotube surface (Rao et al., 2007; Zhang et al., 2013). The results further demonstrate that SWCNT-SH and MWCNT-SH surfaces are effective adsorbents for the removal of Hg(II) ions from polluted water.

**Fig. 7.** Freundlich adsorption isotherm for Hg (II) ions adsorption on (a) pristine SWCNT, (b) pristine MWCNT, (c) SWCNT-COOH, (d) MWCNT-COOH, (e) SWCNT-SH, (f) MWCNT-SH.

The Freundlich adsorption constant K_f and Langmuir constant q_m values for the three adsorbents of SWCNT are ranked as follows: SWCNT-SH > SWCNT-COOH > SWCNT. For the MWCNT adsorbents, the order is MWCNT-SH > MWCNT-COOH > MWCNT. These results indicate that the thiol-derivatized samples exhibit the greatest values for K_f and q_m , while the pure CNT samples have the lowest values for K_f and q_m . The elevated K_f and q_m values for the

thiol-functionalized CNT sample suggest that the adsorption of Hg (II) ions on the CNT-SH surface occurs through a more robust association (chemisorption) compared to other adsorbents (pristine and carboxylic functionalized SWCNT & MWCNT) (Tawabini et al., 2010).

Conclusion

Carbon nanotubes underwent thiol derivatization by sequential carboxylation, reduction, chlorination, and thiolation. The FT-IR, TEM, and SEM analyses demonstrate the presence of carboxylic and thiol groups on the surface of pure CNTs. Adsorption tests under various circumstances indicate that thiol-derivatized SWCNT outperformed all other adsorbents, followed by MWCNT-SH. Analysis of the adsorption isotherm research indicates that the Langmuir model exhibits a superior match to the data compared to the Freundlich isotherm, implying that the adsorption process is monolayer and that all species need equivalent activation energy. The enhanced adsorption capacity of thiol-functionalized carbon nanotubes is attributable to the robust soft acid-soft base interactions between Hg (II) ions and the thiol groups on the nanotube surface. The elevated values of K_f and b for the thiol-functionalized CNT sample suggest that the adsorption of Hg(II) ions on the CNT-SH surface resulted from a more robust interaction (chemisorption) compared to other adsorbents. The results further demonstrate that SWCNT-SH (111.12 mg/g) and MWCNT-SH (83.34 mg/g) surfaces are effective adsorbents for the removal of Hg(II) ions from polluted water.

References

- Abraham TN, Kumar R, Misra RK, et al. (2012) Poly(vinyl alcohol)-based MWCNT hydrogel for lead ion removal from contaminated water. *Journal of Applied Polymer Science* 125(S1):E670–E674. DOI: 10.1002/app.35666.
- Adams L, Oki A, Grady T, et al. (2009) Preparation and characterization of sulfonic acid-functionalized single-walled carbon nanotubes. *Physica E: Low-dimensional Systems and Nanostructures* 41(4):723–728. DOI: 10.1016/j.physe.2008.11.018.
- Ahmad R, Liu X, Wu Y, et al. (2025) N-nitrosodimethylamine removal by a novel silver/sulfur-coated nanoscale zero-valent iron/activated carbon composite: Adsorption kinetics, mechanisms, and degradation pathways. *Separation and Purification Technology* 354:128923. DOI: 10.1016/j.seppur.2024.128923.
- Atieh MA, Bakather OY, Tawabini B, et al. (2010) Effect of carboxylic functional group functionalized on carbon nanotubes surface on the removal of lead from water. *Bioinorganic Chemistry and Applications* 2010:603978. DOI: 10.1155/2010/603978.
- Awabini B, Al-Khaldi S, Atieh M, et al. (2010) Removal of mercury from water by multi-walled carbon nanotubes. *Water Science and Technology* 61(3):591–598.
- Bandaru NM, Nekane R, Habibullah D, et al. (2013) Enhanced adsorption of mercury ions on thiol derivatized single wall carbon nanotubes. *Journal of Hazardous Materials* 261:534–541. DOI: 10.1016/j.jhazmat.2013.07.076.
- Burakov AE, Galunin EV, Burakova IV, et al. (2018) Adsorption of heavy metals on conventional and nanostructured materials for wastewater treatment purposes: A review. *Ecotoxicology and Environmental Safety* 148:702–712. DOI: 10.1016/j.ecoenv.2017.11.034.
- Dada AO (2012) Langmuir, Freundlich, Temkin and Dubinin–Radushkevich isotherms studies of equilibrium sorption of Zn^{2+} onto phosphoric acid modified rice husk. *IOSR Journal of Applied Chemistry* 3(1):38–45. DOI: 10.9790/5736-0313845.
- Dhoble RM, Maddigapu PR, Bhole AG, et al. (2018) Development of bark-based magnetic iron oxide particle (BMiOP), a bio-adsorbent for removal of arsenic (III) from water. *Environmental Science and Pollution Research* 25(20):19657–19674. DOI: 10.1007/s11356-018-1792-x.
- Gowenlock BG and Trotman J (1955) Ultraviolet absorption spectra of some mercury compounds. *Journal of the Chemical Society (Resumed)* 1955:1454–1458. DOI: 10.1039/JR9550001454.
- Hossein S, Nafiseh B and Sohrab A (2013) A new adsorption isotherm model of aqueous solutions on granular activated carbon. *World Journal of Modelling and Simulation* 9(4):243–254.
- Iman M, Esmail S and Mohsen E (2014) Thermodynamics and kinetics of adsorption of Cu(II) from aqueous solutions onto multi-walled carbon nanotubes. *Journal of Saudi Chemical Society* 18(6):792–801. DOI: 10.1016/j.jscs.2011.09.006.
- Kar P and Choudhury A (2013) Carboxylic acid functionalized multi-walled carbon nanotube doped polyaniline for chloroform sensors. *Sensors and Actuators B: Chemical* 183:25–33. DOI: 10.1016/j.snb.2013.03.093.
- Khan MA, Ahmad A, Umar K, et al. (2015) Synthesis, characterization, and biological applications of nanocomposites for the removal of heavy metals and dyes. *Industrial & Engineering Chemistry Research* 54(1):76–82. DOI: 10.1021/ie504148k.

- Kirandeeep and Jeet K (2017) Electrical conductivity of water-based nanofluids prepared with graphene-carbon nanotube hybrid. *Fullerene, Nanotubes and Carbon Nanostructures* 25(12):726–734. DOI: 10.1080/1536383X.2017.1389906.
- Kumar P, Pournara A, Kim K, et al. (2017) Metal-organic frameworks: Challenges and opportunities for ion-exchange/sorption applications. *Progress in Materials Science* 86:25–74. DOI: 10.1016/j.pmatsci.2017.01.002.
- Lim JK, Wan SY, Myung-Han Y, et al. (2003) Selective thiolation of single-walled carbon nanotubes. *Synthetic Metals* 139(2):521–527. DOI: 10.1016/S0379-6779(03)00337-0.
- Lisa YB, Partha J and David AA (2010) Aqueous mercury precipitation with the synthetic dithiolate, BDTH₂. *Fuel* 89(6):1326–1330. DOI: 10.1016/j.fuel.2009.10.031.
- Loganathan P, Vigneswaran S, Kandasamy J, et al. (2014) Removal and recovery of phosphate from water using sorption. *Critical Reviews in Environmental Science and Technology* 44(8):847–907. DOI: 10.1080/10643389.2012.741311.
- Long C, Jung-Hyeon M, Xiaoxin M, et al. (2018) High performance graphene oxide nanofiltration membrane prepared by electrospraying for wastewater purification. *Carbon* 130:487–494. DOI: 10.1016/j.carbon.2018.01.062.
- Maleki MS, Moradi O and Tahmasebi S (2012) Adsorption of albumin by gold nanoparticles: Equilibrium and thermodynamics studies. *Arabian Journal of Chemistry* 243(S1):S1–S7. DOI: 10.1016/j.arabjc.2012.10.009.
- Matlock MM, Howerton BS and Atwood DA (2001) Irreversible precipitation of mercury and lead. *Journal of Hazardous Materials* 84(1):73–82. DOI: 10.1016/S0304-3894(01)00190-X.
- Mojtaba H, Nader B, Habibollah Y, et al. (2014) Adsorption of mercury ions from synthetic and real wastewater aqueous solution by functionalized multi-walled carbon nanotube with both amino and thiolated groups. *Chemical Engineering Journal* 237:217–228. DOI: 10.1016/j.cej.2013.10.014.
- Pacyna EG, Pacyna JM, Sundseth K, et al. (2010) Global emission of mercury to the atmosphere from anthropogenic sources in 2005 and projections to 2020. *Atmospheric Environment* 44(18):2487–2499. DOI: 10.1016/j.atmosenv.2009.06.009.
- Peng W, Li H, Liu Y, Song S, et al. (2017) A review on heavy metal ions adsorption from water by graphene oxide and its composites. *Journal of Molecular Liquids* 230:496–504. DOI: 10.1016/j.molliq.2017.01.064.
- Phothitontimongkol T, Siebers N, Sukpirom N, et al. (2012) Preparation and characterization of novel organo-clay minerals for Hg(II) ions adsorption from aqueous solution. *Applied Clay Science* 43(3–4):343–349. DOI: 10.1016/j.clay.2008.09.016.
- Puri A and Manoj K (2012) A review of permissible limits of drinking water. *Indian Journal of Occupational and Environmental Medicine* 16(1):40–44. DOI: 10.4103/0019-5278.99696.
- Rao G, Lu C and Su F (2007) Sorption of divalent metal ions from aqueous solution by carbon nanotubes: A review. *Separation and Purification Technology* 58(1):224–231. DOI: 10.1016/j.seppur.2006.12.006.
- Rezvani-Boroujeni A, Javanbakht M, Karimi M, et al. (2015) Immobilization of thiol-functionalized nanosilica on the surface of poly(ether sulfone) membranes for the removal of heavy-metal ions from industrial wastewater samples. *Industrial & Engineering Chemistry Research* 54(1):502–513. DOI: 10.1021/ie504106y.
- Samani MR, Ebrahimbabaie P and Molamahmood HV (2016) Hexavalent chromium removal by using synthesis of polyaniline and polyvinyl alcohol. *Water Science and Technology* 74(10):2305–2313. DOI: 10.2166/wst.2016.412.
- Shadbad MJ, Ali M and Ataallah S (2011) Mercury(II) removal from aqueous solutions by adsorption on multi-walled carbon nanotubes. *Korean Journal of Chemical Engineering* 28(4):1029–1034. DOI: 10.1007/s11814-010-0463-5.
- Stafiej A and Pyrzynska K (2007) Adsorption of heavy metal ions with carbon nanotubes. *Separation and Purification Technology* 58(1):49–52. DOI: 10.1016/j.seppur.2007.07.008.
- Tan I and Hameed B (2010) Adsorption isotherms, kinetics, thermodynamics and desorption studies of basic dye on activated carbon derived from oil palm empty fruit bunch. *Journal of Applied Sciences* 10(21):2565–2571. DOI: 10.3923/jas.2010.2565.2571.
- Verma NK (2015) Study on the controlled growth of lanthanum hydroxide and manganese oxide nano composite under the presence of cationic surfactant. *Applied Medical Informatics* 4(1):11–15. DOI: 10.11648/JAM.20150401.13.
- Yardim MF, Budinova T, Ekinci E, et al. (2003) Removal of mercury (II) from aqueous solution by activated carbon obtained from furfural. *Chemosphere* 52(5):835–841. DOI: 10.1016/S0045-6535(03)00267-4.
- Zeng B, Wang W, He S, et al. (2021) Facile synthesis of zinc based organic framework for aqueous Hg(II) removal: Adsorption performance and mechanism. *Nano Materials Science* 3(4):429–439. DOI: 10.1016/j.nanoms.2021.06.005.

Zhang S, Yuanyuan Z, Junshen L, et al. (2013) Thiol modified $\text{Fe}_3\text{O}_4@\text{SiO}_2$ as a robust, high effective, and recycling magnetic sorbent for mercury removal. *Chemical Engineering Journal* 226:30–38. DOI: 10.1016/j.cej.2013.04.060.

Author Contributions

KJ conceptualized the study and designed the methodology. NG carried out the experiments and prepared the original draft of the manuscript. KJ performed the data analysis and reviewed and edited the manuscript.

Acknowledgements

The authors gratefully acknowledge the Electron Microscopy and Nanoscience Laboratory and the Department of Mathematics, Statistics & Physics, Punjab Agricultural University, Ludhiana, for providing financial support and the necessary infrastructure to carry out this research.

Funding

Not applicable.

Availability of data and materials

Not applicable.

Competing interest

The authors declare no competing interests.

Ethics approval

Not applicable.



Open Access *This article is licensed under a Creative Commons Attribution 4.0 International License, which permits use, sharing, adaptation, distribution, and reproduction in any medium or format, as long as you give appropriate credit to the original author(s) and the source, provide a link to the Creative Commons license, and indicate if changes were made. The images or other third-party material in this article are included in the article's Creative Commons license unless indicated otherwise in a credit line to the material. If material is not included in the article's Creative Commons license and your intended use is not permitted by statutory regulation or exceeds the permitted use, you will need to obtain permission directly from the copyright holder. Visit for more details <http://creativecommons.org/licenses/by/4.0/>.*

Citation: Garg N and Jeet K (2026) Isotherm Modeling and Thermodynamic Investigation of Mercury Adsorption on Functionalized Carbon Nanotubes: A Comparative Study of SWCNTs and MWCNTs. *Environmental Science Archives* 5(1): 178-190.